JACS
JOURNAL OF THE AMERICAN CHEMICAL SOCIETY

Communication

pubs.acs.org/JACS

Theoretical Modeling of Plasmon-Enhanced Raman Images of a Single Molecule with Subnanometer Resolution

Sai Duan,[†,‡] Guangjun Tian,[‡] Yongfei Ji,[‡] Jiushu Shao,[§] Zhenchao Dong,[†] and Yi Luo*[,†,‡]

[†]Hefei National Laboratory for Physical Science at the Microscale and Synergetic Innovation Center of Quantum Information & Quantum Physics, University of Science and Technology of China, Hefei, Anhui 230026, P. R. China

[‡]Department of Theoretical Chemistry and Biology, School of Biotechnology, Royal Institute of Technology, S-106 91 Stockholm, Sweden

[§]Key Laboratory of Theoretical Computational Photochemistry, Ministry of Education, College of Chemistry, Beijing Normal University, Beijing 100875, P. R. China

Supporting Information

ABSTRACT: Under local plasmonic excitation, Raman images of single molecules can now surprisingly reach subnanometer resolution. However, its physical origin has not been fully understood. Here we report a quantum-mechanical description of the interaction between a molecule and a highly confined plasmonic field. We show that when the spatial distribution of the plasmonic field is comparable to the size of the molecule, the optical transition matrix of the molecule becomes dependent on the position and distribution of the plasmonic field, resulting in a spatially resolved high-resolution Raman image of the molecule. The resonant Raman image reflects the electronic transition density of the molecule. In combination with first-principles calculations, the simulated Raman image of a porphyrin derivative adsorbed on a silver surface nicely reproduces its experimental counterpart. The present theory provides the basic framework for describing linear and nonlinear responses of molecules under highly confined plasmonic fields.

The development of the tip-enhanced Raman scattering (TERS)[1] technique has significantly increased the spatial resolution of Raman images of molecules.[2−9] Under low-temperature and ultrahigh-vacuum conditions, the resolution has amazingly reached the subnanometer level for a porphyrin derivative adsorbed on a silver surface.[8] It is anticipated that the spatial confinement of the tip-induced plasmon plays a decisive role in achieving such high resolution. In this case, the spatial distribution of the plasmonic field has to be comparable to the size of the molecule, even with the inclusion of possible nonlinear processes.[8,10] This situation presents a great challenge to conventional response theory, which always assumes that the electromagnetic field uniformly interacts with the molecule.[11−18] A new theory that takes into account the locality of the plasmonic field thus needs to be developed. Moreover, how to model a Raman image and what a Raman image really tells about the molecular structure are important issues that have not yet been addressed in the literature.

Here we present a new theory to describe Raman images of molecules as observed in TERS experiments. The interaction between the molecule and the plasmonic field is described quantum-mechanically. In combination with first-principles calculations, we have successfully reproduced the experimental Raman image of a porphyrin derivative adsorbed on a silver surface.[8] It was found that within the Born−Oppenheimer approximation, the resonant Raman image reflects the density of the electronic transition between the ground and excited states. The effects of linear and nonlinear processes on the resolution of the Raman images have been identified.

In TERS experiments, a nanocavity formed between the tip and the substrate is the host of the spatially confined plasmon (SCP). For the metals used in the experiments, the plasmonic frequency often falls into the visible or UV−vis region, and hence, the electric dipole approximation[16] can still hold. The interaction Hamiltonian between the SCP and the adsorbates can be described by[16] $\hat{H} = -e\hat{\mathbf{r}}\cdot\hat{\mathbf{E}}(\mathbf{r}, \mathbf{R}_T, t)$, where e is the elementary charge, $\hat{\mathbf{r}}$ is the electron position operator, and $\hat{\mathbf{E}}$ is the operator for the electric field of the SCP, which is obviously related to the tip position $\mathbf{R}_T$. In this case, $\hat{\mathbf{E}}$ cannot be treated uniformly in space because of its specific spatial distribution. Consequently, the optical transition matrix element between the electronic ground state $|\psi_g\rangle$ and the electronic excited state $|\psi_r\rangle$ is given by $\langle\psi_g|\hat{\mathbf{r}}\cdot\hat{\mathbf{E}}(\mathbf{r}, \mathbf{R}_T)|\psi_r\rangle$ rather than $\langle\psi_g|\hat{\mathbf{r}}|\psi_r\rangle\cdot\mathbf{E}$ as in conventional response theory.[11,14] This modification implies that the optical processes are dependent on the position of the tip that hosts the SCP. This can naturally explain why it is possible to obtain superhigh spatial resolution in the Raman images.

By taking into account the position-dependent electric field, we can rederive the expressions for the linear and nonlinear resonant Raman processes following Albrecht's theory[11,17] and the theory of femtosecond stimulated Raman spectroscopy proposed by Lee et al.,[14] respectively (see the Supporting Information (SI) for details). The Raman intensities can be calculated from the amplitude of the induced polarization as a sum of Franck−Condon (FC) and Herzberg−Teller (HT) terms (eqs S6−S8 and S16−S18 in the SI). By using Gaussian functions to represent the spatial distribution of the SCP, we can compute the Raman images of a single *meso*-tetrakis(3,5-di-*tert*-butylphenyl)porphyrin (H_2TBPP) molecule adsorbed on the Ag(111) surface, which were measured in a recent study.[8]

Received: April 10, 2015
Published: July 17, 2015

DOI: 10.1021/jacs.5b03741
J. Am. Chem. Soc. 2015, 137, 9515−9518

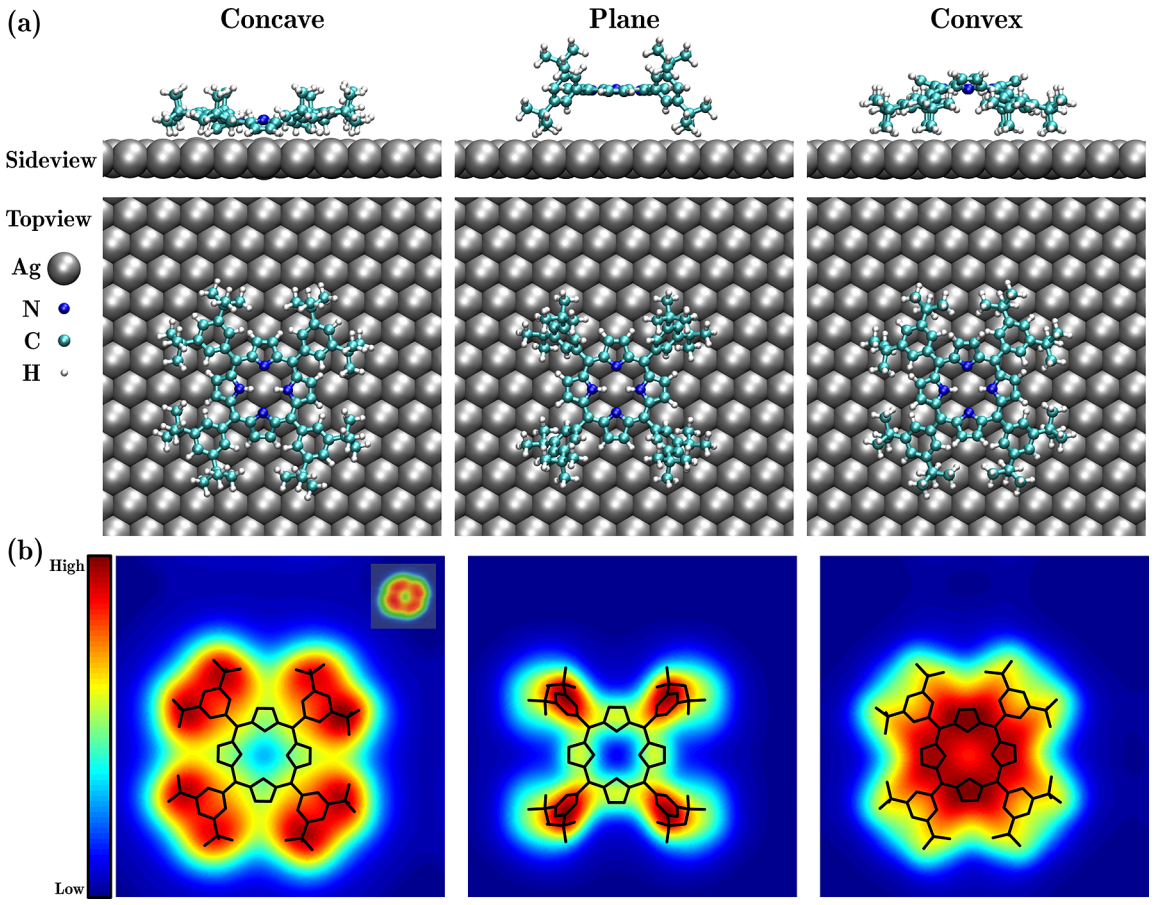

Figure 1. (a) Optimized structures of one H_2TBPP tautomer adsorbed on the Ag(111) surface in the (left) concave, (center) plane, and (right) convex configurations. Gray, blue, cyan, and white balls represent Ag, N, C, and H atoms, respectively. For clarity, only the topmost slab layer of the Ag(111) surface and all of the adsorbate atoms in one supercell are depicted. (b) Calculated average STM images with the sample biased by 1.0 V for the (left) concave, (center) plane, and (right) convex configurations. The solid lines represent the skeleton of H_2TBPP. The inset in the left panel shows the experimental STM image under the same conditions.[8]

We first calculated the most stable configuration of H_2TBPP on the Ag(111) surface. Here we considered two degenerate tautomers of the H_2TBPP molecule (Figure S1 in the SI).[19] The optimized structures of one H_2TBPP tautomer adsorbed on the Ag(111) surface are depicted in Figure 1a. The optimized structures of the other tautomers are similar, but the central hydrogen atoms are bonded to different nitrogen atoms. We considered three different configurations, namely, concave, plane, and convex. The first and last configurations were identified when H_2TBPP adsorbed on the Cu(111) surface was studied by scanning tunneling microscopy (STM),[20] and the second configuration is the minimum of the isolated molecule.[21] Our energy calculations showed that the concave configuration is the most stable one when long-range dispersion[22] is considered, while the convex configuration is the least stable one. From the calculated STM images and the experimental result[8] (Figure 1b), one can immediately notice that only the calculated STM image of the concave configuration resembles the experimental counterpart. It can thus be firmly concluded that H_2TBPP adopts the concave configuration when adsorbed on the Ag(111) surface under the experimental conditions.

Under the resonant condition, for allowed transitions, the linear Raman intensity is known to be dominated by the FC term.[23] For the FC term, the linear Raman images for the different modes are the same because the electronic part of the FC term provides only a universal contribution to all of the modes (eq S7). The simulated linear Raman images from the FC term are presented in Figure 2. It can be seen that the size of the Raman image is closely associated with the size of the SCP. This implies that the precondition for the high-resolution Raman image is the generation of a highly focused plasmonic field. It is quite encouraging to observe that different configurations of the molecule can generate very different Raman images, indicating TERS is a powerful tool to study the structure of adsorbates. One can notice that the Raman image of the concave configuration with a full width at half-maximum (fwhm) of 20 Å is in very good agreement with the experimental image, which is consistent with the energy and STM image calculations. Here the symmetry breaking of the calculated Raman images is caused by the local interaction between the adsorbate and the Ag(111) substrate. By definition, Raman images reflect the density change involved in the electronic transition rather than the local density of states of the adsorbate. We should mention that the calculated resonant Raman spectrum for the concave configuration is also in good agreement with the experimental observations (Figure S2).

The HT term is dependent on the vibrational modes, and its contribution can thus be used to identify the vibrations of the molecule. We evaluated the effect of the HT term for two vibrational bands (at around 820 and 1200 cm^{-1}) using the linear coupling model.[24] The calculated Raman images from the total linear polarization as well as the HT term alone for these two bands are shown in Figure 3. As expected, the HT term is indeed

DOI: 10.1021/jacs.5b03741
J. Am. Chem. Soc. 2015, 137, 9515−9518

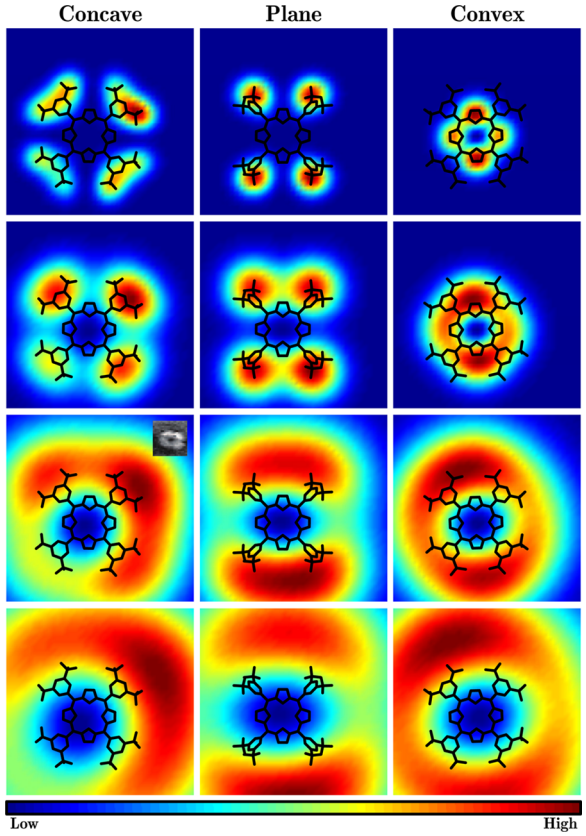

Figure 2. Calculated linear Raman images from the FC term with the full width at half-maximum (fwhm) of the x and y components set at (top to bottom) 5, 10, 20, and 30 Å for (left to right) the concave, plane, and convex configurations. The solid lines represent the skeleton of H_2TBPP. The inset shows the experimental Raman image.[8]

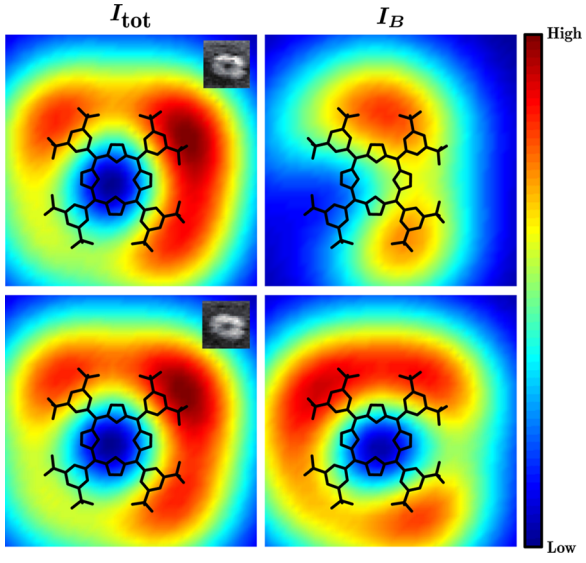

Figure 3. Calculated linear Raman images of vibrational bands at (top) 820 and (bottom) 1200 cm^{-1} from (left) total polarization (I_{tot}) and (right) only the HT term (I_B) with an fwhm of 20 Å for the concave configuration. I_B was scaled by factors of 100 and 400 for 800 and 1200 cm^{-1}, respectively. The solid lines represent the skeleton of H_2TBPP. The insets show the corresponding experimental Raman images.[8]

very sensitive to the vibrational modes. Its contribution to the total intensity holds the key to distinguishing Raman images of different vibrations. However, under the resonant condition, the contribution of the HT term is often small,[23] which is unfortunately also the case for the H_2TBPP molecule. This should be attributed to the geometrical distortion in the concave configuration, which results in a larger electronic dipole transition moment to the state at around 530 nm. In this case, the A term can become dominant. Hence, the Raman images from the total intensity calculations appear to be identical for the two vibrational bands. We note that the calculated Raman images given in ref 8 were obtained by assuming that the confined plasmonic field does not alter the transition matrix itself, which is a very crude approximation to the basic theory presented here.

It was found experimentally that the observed Raman intensity was nonlinearly dependent on the power of the incident light.[8] The linear and nonlinear processes were found to contribute 40% and 60%, respectively, of the total intensity under the saturation condition.[8] It is thus necessary to examine how the nonlinear process affects the Raman image of the molecule. Three processes, namely, the stimulated Raman process as well as two hot luminescence processes (I and II), can contribute to the nonlinear Raman signal when both pump and broadband SCPs are involved. In analogy to the theory proposed by Lee et al.,[14] the amplitude of the induced nonlinear polarization also consists of FC and HT terms (eqs S16−S18).

Similar to the linear process, the FC term is also completely dominant in the nonlinear process. The calculated nonlinear Raman images with fwhm of 20 Å are depicted in the top panel of Figure 4. In general, the nonlinear images do have higher spatial

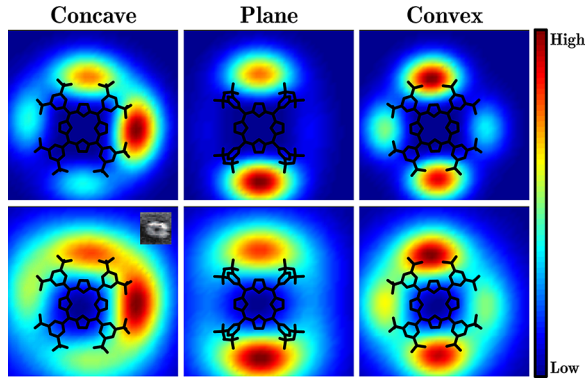

Figure 4. Calculated (top) nonlinear and (bottom) total Raman images for (left to right) the concave, plane, and convex configurations under a plasmonic field with an fwhm of 20 Å. The solid lines represent the skeleton of H_2TBPP. The inset shows the experimental Raman image.[8]

resolution than their linear counterparts. However, for this particular system, the improvement is not as much as one anticipated[8] because of the mixture of the linear and nonlinear contributions. The calculated total Raman image (including both linear and nonlinear effects) from the concave configuration with the field distribution size of 20 Å gives the best agreement with the experimental image, as shown in the bottom panel of Figure 4. This result reveals that the actual size of the experimentally confined plasmonic field could be close to 20 Å. This argument is supported by recent advanced theoretical modeling studies.[25−27] Simulations using the finite-element method for realistic STM setups[25,26] revealed that the spatial extent of the electric field can be around 2 nm. Upon inclusion of the molecular self-interaction, the size of the plasmonic field was found to be further reduced.[27] From current simulations, the size of the SCP seems to play the decisive role in the subnanometer Raman

DOI: 10.1021/jacs.5b03741
J. Am. Chem. Soc. 2015, 137, 9515−9518

images. However, the increase in the nonlinear contribution to the total intensity is on the other hand an effective way to further improve the resolution of the Raman image.

We note that the present consideration of the SCP is equivalent to the quantization scheme proposed by Archambault et al.[28,29] for the propagation of surface plasmonic waves as well as the classical treatment proposed by Xu and co-workers.[30,31] However, the key difference is that because of the size of the SCP, we have to keep the distribution function inside the optical transition matrix element. Besides, according to the definition, the first-order Taylor expansion for $\mathbf{E}(\mathbf{r}, \mathbf{R}_T)$ would lead to electric field gradient effects in Raman spectroscopy (or the so-called quadruple Raman), as discussed in the literature.[25,26,32,33] However, we should stress that with such a highly confined field employed in the modeling of the images, the use of the gradient term alone could not well describe the plasmonic field. Therefore, the higher-order terms have to be included. We also note that the current theory can be connected to the time-dependent Kohn−Sham approach in real space for a highly confined electromagnetic field.[34]

It should be mentioned that the Raman calculations were performed for a single molecule. Inclusion of the substrate might increase the contribution of the HT term, which could be a reason for the small variation observed in the experimental Raman images of different vibrational modes.[8] A feasible way to significantly increase the contribution of the HT term would be to adopt the nonresonant Raman scattering scheme, which requires better sensitivity of the measurements. Furthermore, one may expect to use the linear effect only for the Raman images, which can avoid destruction of the molecule by the high intensity of the plasmonic field.

In summary, we have proposed a quantum-mechanical description of the interaction between a molecule and a highly confined plasmonic field. It shows that the SCP can modify the transition matrix, resulting in high-resolution Raman images. The usefulness of the description is highlighted by the successful reproduction of the experimental Raman images of a H_2TBPP molecule adsorbed on the Ag(111) surface. The theoretical framework established here lays the foundation for the future development of linear and nonlinear plasmonic spectroscopy. We also expect applications of the current theory in chemistry, material science, physics, and biology.

■ ASSOCIATED CONTENT

Supporting Information

Theoretical background and additional data. The Supporting Information is available free of charge on the ACS Publications website at DOI: 10.1021/jacs.5b03741.

■ AUTHOR INFORMATION

Corresponding Author

*yiluo@ustc.edu.cn

Notes

The authors declare no competing financial interest.

■ ACKNOWLEDGMENTS

This work was supported by the Ministry of Science and Technology of China (2010CB923300), the National Natural Science Foundation of China (21121003), the Strategic Priority Research Program of the Chinese Academy of Sciences (XDB01020200), the Göran Gustafsson Foundation for Research in Natural Sciences and Medicine, and the Swedish Research Council (VR). Computer time from the Swedish National Infrastructure for Computing (SNIC) is acknowledged.

■ REFERENCES

(1) (a) Stöckle, R. M.; Suh, Y. D.; Deckert, V.; Zenobi, R. *Chem. Phys. Lett.* **2000**, *318*, 131−136. (b) Anderson, M. S. *Appl. Phys. Lett.* **2000**, *76*, 3130−3132. (c) Hayazawa, N.; Inouye, Y.; Sekkat, Z.; Kawata, S. *Opt. Commun.* **2000**, *183*, 333−336. (d) Pettinger, B.; Pucardi, G.; Schuster, R.; Ertl, G. *Electrochem. (Tokyo, Jpn.)* **2000**, *68*, 942−949.

(2) Hartschuh, A.; Sánchez, E. J.; Xie, X. S.; Novotny, L. *Phys. Rev. Lett.* **2003**, *90*, 095503.

(3) Anderson, N.; Hartschuh, A.; Cronin, S.; Novotny, L. *J. Am. Chem. Soc.* **2005**, *127*, 2533−2537.

(4) Steidtner, J.; Pettinger, B. *Phys. Rev. Lett.* **2008**, *100*, 236101.

(5) Ichimura, T.; Fujii, S.; Verma, P.; Yano, T.; Inouye, Y.; Kawata, S. *Phys. Rev. Lett.* **2009**, *102*, 186101.

(6) Yano, T.-a.; Verma, P.; Saito, Y.; Ichimura, T.; Kawata, S. *Nat. Photonics* **2009**, *3*, 473−477.

(7) Stadler, J.; Schmid, T.; Zenobi, R. *Nano Lett.* **2010**, *10*, 4514−4520.

(8) Zhang, R.; Zhang, Y.; Dong, Z. C.; Jiang, S.; Zhang, C.; Chen, L. G.; Zhang, L.; Liao, Y.; Aizpurua, J.; Luo, Y.; Yang, J. L.; Hou, J. G. *Nature* **2013**, *498*, 82−86.

(9) Chen, C.; Hayazawa, N.; Kawata, S. *Nat. Commun.* **2014**, *5*, 3312.

(10) Atkin, J. M.; Raschke, M. B. *Nature* **2013**, *498*, 44−45.

(11) Albrecht, A. C. *J. Chem. Phys.* **1961**, *34*, 1476−1484.

(12) Neugebauer, J.; Reiher, M.; Kind, C.; Hess, B. A. *J. Comput. Chem.* **2002**, *23*, 895−910.

(13) Masiello, D. J.; Schatz, G. C. *Phys. Rev. A: At., Mol., Opt. Phys.* **2008**, *78*, 042505.

(14) Lee, S.-Y.; Zhang, D.; McCamant, D. W.; Kukura, P.; Mathies, R. A. *J. Chem. Phys.* **2004**, *121*, 3632−3642.

(15) Sakurai, J. J. *Advanced Quantum Mechanics*; Addison-Wesley: Reading, MA, 1967.

(16) Scully, M. O.; Zubairy, M. S. *Quantum Optics*, 1st ed.; Cambridge University Press: Cambridge, U.K., 1997.

(17) Long, D. A. *The Raman Effect: A Unified Treatment of the Theory of Raman Scattering by Molecules*; Wiley: Chichester, U.K., 2002.

(18) le Ru, E.; Etchegoin, P. *Principles of Surface-Enhanced Raman Spectroscopy and Related Plasmonic Effects*, 1st ed.; Elsevier: Amsterdam, 2009.

(19) Fu, Q.; Yang, J.; Luo, Y. *Appl. Phys. Lett.* **2009**, *95*, 182103.

(20) Ditze, S.; Stark, M.; Buchner, F.; Aichert, A.; Jux, N.; Luckas, N.; Görling, A.; Hieringer, W.; Hornegger, J.; Steinrück, H.-P.; Marbach, H. *J. Am. Chem. Soc.* **2014**, *136*, 1609−1616.

(21) Aydin, M. *Vib. Spectrosc.* **2013**, *68*, 141−152.

(22) Grimme, S. *J. Comput. Chem.* **2006**, *27*, 1787−1799.

(23) Myers Kelley, A. *J. Phys. Chem. A* **2008**, *112*, 11975−11991.

(24) Macak, P.; Luo, Y.; Ågren, H. *Chem. Phys. Lett.* **2000**, *330*, 447−456.

(25) Sun, M.; Zhang, Z.; Chen, L.; Sheng, S.; Xu, H. *Adv. Opt. Mater.* **2014**, *2*, 74−80.

(26) Meng, L.; Yang, Z.; Chen, J.; Sun, M. *Sci. Rep.* **2015**, *5*, 9240.

(27) Zhang, C.; Chen, B.-Q.; Li, Z.-Y. *J. Phys. Chem. C* **2015**, *119*, 11858−11871.

(28) Archambault, A.; Marquier, F.; Greffet, J.-J.; Arnold, C. *Phys. Rev. B: Condens. Matter Mater. Phys.* **2010**, *82*, 035411.

(29) Tame, M. S.; McEnery, K. R.; Özdemir, Ş. K.; Lee, J.; Maier, S. A.; Kim, M. S. *Nat. Phys.* **2013**, *9*, 329−340.

(30) Xu, H.; Wang, X.-H.; Persson, M. P.; Xu, H. Q.; Käll, M.; Johansson, P. *Phys. Rev. Lett.* **2004**, *93*, 243002.

(31) Johansson, P.; Xu, H.; Käll, M. *Phys. Rev. B: Condens. Matter Mater. Phys.* **2005**, *72*, 035427.

(32) Sass, J. K.; Neff, H.; Moskovits, M.; Holloway, S. *J. Phys. Chem.* **1981**, *85*, 621−623.

(33) Ayars, E. J.; Hallen, H. D.; Jahncke, C. L. *Phys. Rev. Lett.* **2000**, *85*, 4180−4183.

(34) Iwasa, T.; Nobusada, K. *Phys. Rev. A: At., Mol., Opt. Phys.* **2009**, *80*, 043409.

DOI: 10.1021/jacs.5b03741
J. Am. Chem. Soc. 2015, 137, 9515−9518